Save

LA-UR-84:1725

Los Alamos National Laboratory is operated by the University of California for the United States Department of Energy under contract W-7405-ENG-36

TITLE: PATTERN SELECTION AND LOW-DIMENSIONAL CHAOS IN DISSIPATIVE MANY DEGREE-OF-FREEDOM SYSTEMS

AUTHOR(S): A. R. Bishop
J. E. Eilbeck
I. Satija
G. Wysin

SUBMITTED TO: Physical Review Letters

Lectures Appl. Math 23 125 (1986)

Los Alamos National Laboratory
Los Alamos, New Mexico 87545

FORM NO 836 R4
ST NO 2629 5/81

PATTERN SELECTION AND LOW-DIMENSIONAL CHAOS IN DISSIPATIVE MANY DEGREE-OF-FREEDOM SYSTEMS

A. R. Bishop, J. C. Eilbeck,[†] I. Satija[*] and G. Wysin[††]

Center for Nonlinear Studies

and Theoretical Division

Los Alamos National Laboratory

Los Alamos, NM 87545, USA

ABSTRACT

The long time behavior of a number of driven dissipative nonlinear systems, with many degrees of freedom, can be characterized by a small number of dominating modes. These modes are responsible for the low dimension of the strange attractor in the chaotic regime, as estimated by the Grassberger and Procaccia algorithm. While in the chaotic regime these systems can nevertheless exhibit coherent spatial structures, reflecting a strong mode-locking between the underlying normal modes of the unperturbed system.

In recent years considerable attention has been given to the properties of low-dimensional maps as models for complicated dynamics in higher-dimensional dynamical systems.[1] This attention has been merited by the proof of "universal" properties in classes of one-dimensional maps.[1] However, with few exceptions, the low-dimensionality has been introduced explicitly by restricting consideration to models with a very small number of degrees-of-freedom. On the other hand, equally active research has focused on the subject of spatial pattern selection in non-equilibrium nonlinear systems with many degrees-of-freedom (e.g. convection cells,[2] reaction-diffusion systems[3]). In these cases mode-locking is very strong and a small number of modes dominate the spatial structure and temporal evolution in a nonlinear partial differential equation (p.d.e.) or large system of coupled ordinary differential equations (o.d.e.'s).

The perspective we wish to emphasize in this report is that the two phenomena of pattern formation and low-dimensional chaos are intimately connected in perturbed, dissipative dynamical systems with many degrees-of-freedom. More specifically, chaotic dynamics can develop by chaotic motions of the collective coordinates identifying the dominant (determining) patterns in the quiescent regimes. In this way only a small loss of mode-locking is responsible for the temporal chaos which can coexist with spatial coherence.

There are many examples of this scenario,[4] which gives the problem of identifying and testing (nonlinear)[5] mode reduction schemes a general importance. We have chosen to concentrate here on a set of driven and damped nonlinear partial differential equations (and their discrete analogs) in one spatial dimension. In all of these cases, coherent nonlinear modes ("solitons" or near-solitons[6]) are fundamental excitations

of the underlying unperturbed Hamiltonian system. Detailed results for a number of examples will be presented elsewhere.[7,8] Here we will merely abstract typical cases from five examples so as to illustrate the interconnectedness of pattern selection, low-dimensional chaos, and coexisting coherence and chaos.

Four of our examples are based on perturbed sine-Gordon (SG) equations

$$\phi_{tt} - \phi_{xx} + \sin \phi = F(x,t) - \varepsilon\phi_t \quad . \tag{1}$$

Here ϕ is a scalar field and x, t are space and time, respectively. Subscripts denote derivates. $F(x,t)$ is a forcing field and ε a damping constant. In the four examples below we have studied eqn. (1) numerically on a finite line (length L) and with a high density spatial mesh (approximating the p.d.e.):

Case A. Here $L = 24$ with 120 grid points and periodic boundary conditions, $\varepsilon = 0.2$ and $F(x,t) = \gamma \sin \omega_d t$ with $\omega_d = 0.6$. The initial data is a static "pulse" profile (the actual shape of the pulse is not very important -- there is a large basin of initial data with the same attractor[7]). As reported elswhere,[7] this system undergoes a spontaneous spatial period doubling for $0.6 \lesssim \gamma \lesssim 0.9$ but remains simply periodic in time. Typical spatial profiles are shown in Fig. 1a, and should be thought of as "breather-soliton" wavetrains.[6,7,9] As $\gamma \stackrel{\sim}{\to} 0.9$, the duration of a "chaotic" initial transient diverges, resulting in temporal chaos for $0.9 \lesssim \gamma \lesssim 1.4$. (Diagnostics for chaos are discussed in ref. 7). Accompanying this chaos are large ($>> 2\pi$) variations in the spatial average of $\phi(x,t)$ [denoted by $\bar{\phi}(t)$] and large amplitude ($\sim 2\pi$) spatial variations in ϕ relative to $\bar{\phi}$. Instantaneous spatial correlation functions suggest strong structural disorder unless the functions of ϕ being correlated are selected carefully (e.g. cos).

However, following the evolution in detail through a period of the driving field (Fig. 1b) shows transparently that the basic coherent structures in the quiescent pre-chaotic regime are preserved, but that their mode-locking relative to each other has been (chaotically) broken so that the structure fails to repeat by a small amount after each driver period. Consequently, we can decompose the field at each instant of time into either two "breather solitons" or two "kink-solitons" and two "antikink-solitions" (at instants of kink-antikink collision the field ϕ may appear to be flat -- see Fig. 1b). Furthermore, chaotic evolution of $\bar{\phi}(t)$ through multiples of 2π does not take place via single particle dynamics but rather through the slow diffusion of the kink (antikink) solitons -- as with thermally assisted transport in such systems.

We have confirmed the identification of the small number of coherent "soliton" modes in the chaotic regime by projecting the field at successive times onto a true solition basis[6] -- the optimal modes for the unperturbed system (1). Results are described elsewhere[10] but fully support the strong implications of Fig. 1. This small number of dominating collective modes suggests that the chaos will be governed by a low-dimensional strange attractor.[11] We have checked the dimension (ν) using the algorithm proposed by Grassberger and Procaccia.[12] We estimate[12] that $\nu(\gamma = 1.0) = 2.5 \pm 0.3$, and in fact the dimension is found to lie within this range throughout the chaotic regime. Thus ν is indeed low.[13] [For $\gamma \lesssim 0.9$, ν is 1.0, as expected. ν also approaches 1.0 for large $\gamma \gtrsim 10$ where the nonlinear potential is a small perturbation on the dynamics.]

Case B. Here conditions are the same as case A, except that the initial data is a single static kink with periodic boundary conditions mod (2π). The attractor is found[7] to be kink plus a "breather" and for $\gamma \gtrsim 0.9$,

these coherent structures move randomly with respect to each other producing temporal chaos. The dimension of the chaos is again correspondingly low: e.g., for $\gamma = 1.0$, we estimate[12] $\nu = \pm 2.6 \pm 0.5$.

Case C. Here[8] we adopted boundary conditions appropriate to a finite Josephson junction oscillator in zero magnetic field,[14] viz. $\phi_x(x = 0,t) = \phi_x(x = L,t) = 0$. The number of grid points = 120, $L = 6$, $\varepsilon = 0.1$, and $F(x,t) = \gamma_0 + \gamma \sin \omega_d t$ with $\gamma_0 = 0.35$. Even with single kink initial conditions i.e. on the first "zero field step" (ZFS)[14] a great variety of dynamical behaviors (including jumping between ZFS's) are observed.[8] For our present purposes we report an example which illustrates a prevalent source of chaos: for $\omega_d = 1.25$ and $\gamma = 1.2$, the kink initial data is attracted to a nonchaotic "symmetric" state[14] on the third ZFS as shown in Fig. 2a. Increasing γ to 1.5, we find a chaotic long-time evolution in which the strongly mode-locked coherent structures of the third ZFS are still dominant but their relative mode-locking has been (chaotically) broken -- see Fig. 2b. Consistently, we estimate[12] the attractor dimension to be low: $\nu = 2.5 \pm 0.4$.

Case D. In this case[7] we used outflow boundary conditions, $L = 40$, 800 grid points $\varepsilon = 0.05$, and completely flat initial data ($\phi(x,t = 0) = \phi_t(x,t = 0) = 0$. Chaotic evolution is induced by choosing a spatially inhomogeneous driving field $F(x,t) = \gamma$, $x \in [15,25]$, $F(x,t) = 0$ elsewhere. Our estimates of ν for $0 \leq \gamma \leq 5$ show that ν increases from 1 at $\gamma = 0$ to 2.8 ± 0.4 for $\gamma = 2$ (with a rapid increase at the chaotic threshold $\gamma \simeq 0.4$) and then decreases to 1 at larger values of γ (as in Case A). Again the low dimension is entirely consistent with an examination of spatial profiles: once more ϕ evolves by the separation of coherent kink-antikink pairs which are periodically nucleated at the center of the line.[7]

Examples A-D are all based on perturbations of the SG system, although with a great variety of initial data, boundary conditions and perturbations. The perturbations are sufficiently strong that this choice is not a limitation on the general phenomena we have described. In particular, the near integrability of the unperturbed Hamiltonian system plays no role. To emphasize this, we consider a non-integrable, two-component field example in:

Case E. Here we studied[8] a strongly perturbed magnetic chain of classical spins $\vec{S}_n = (S_n^x, S_n^y, S_n^z) = (\cos\theta_n \cos\phi_n, \cos\theta_n \sin\phi_n, \sin\theta_n)$, $n = 1, 2, 3 \ldots N$, governed by the Hamiltonian

$$H = -\sum_{n=1}^{N} \vec{S}_n \cdot \vec{S}_{n+1} + \alpha \sum_{n=1}^{N} S_n^{z\,2} - \vec{B} \cdot \sum_{n=1}^{N} \vec{S}_n \quad , \tag{2}$$

where $\alpha > 0$ is an easy-plane anisotropy (ϕ_n and θ_n are the in-plane and out-of-plane angles) and $\vec{B}$ is an applied magnetic field. A Gilbert-Landau dissipation term[8] of strength ε is added to the equations of motion following from (2). Again a great variety of chaotic and non-chaotic evolutions are possible,[18] depending on magnetic field configurations and parameter values. However, spontaneous pattern formation, consequent low-dimensional chaos, and coexisting coherence and chaos are once again prevalent phenomena. An example is illustrated in Fig. 3. Here we have used periodic boundary conditions, $N = 150$, $\varepsilon = 0.1$, $\alpha = 0.1907$, $\vec{B} = (B^x, B^y, B^z) = (B_0^x \sin(\omega_d t), 0, 0)$, $\omega_d = 0.05144$, and random initial data $\phi_n(t = 0)$, $\theta_n(t = 0)$. In Fig. 3a, $B_0^x = 0.03429$. The period-½ spatial structure

seen in Fig. 3a forms spontaneously as the long time attractor with simply-periodic entrained motion. Decreasing B_0^x to 0.02743 we have entered a chaotic regime characterized (Fig. 3b) by chaotic motions of the coherent nonlinear mode components of the precursor period-½ spatial pattern. The Grassberger-Procaccia estimate[12] of the attractor dimension is correspondingly low -- for $B_0^x = 0.02743$, we find $\nu = 1.7 \pm 0.4$ for S^y and $\nu = 1.9 \pm 0.4$ for S^z.

In conclusion, we shown in a large variety of driven, dissipative p.d.e.'s that a small number of determining modes are typically responsible both for spontaneous pattern formation in quiescent regimes and for low-dimensional chaos in subsequent chaotic regimes. Thus coexisting coherence and chaos is a natural corollary. The identification of determining nonlinear modes clearly motivates the choice and study of specific truncated systems of coupled o.d.e.'s to be compared with the dynamics of the full p.d.e.'s. These studies are in progress.

We are grateful for useful conversations with D. W. McLaughlin and A. C. Newell. One of us (JCE) would like to acknowledge the Royal Society of London for partial financial support during the period while this work was carried out, and the U.S./U.K. Education Commission and the Carnegie Trust (Edinburgh) for further travel grants.

References

† Permanent address: Department of Mathematics, Heriot-Watt University, Riccarton, Edinburgh EH14 4AS, UK.

* Present address: Bartol Research Institute, University of Delaware, Newark, DE 19711, USA.

†† Permanent address: LASSP, Clark Hall, Cornell University, Ithaca, NY 14853, USA.

1. See articles in Physica 7D (1983).

2. e.g. M. Cross, Phys. Rev. A25, 1065 (1982).

3. e.g. H. Meinhardt, "Models of Biological Pattern Formation" (Academic Press 1982).

4. Examples of coexisting coherence and chaos include clumps and cavitons in turbulent plasmas and large scale structures in turbulent fluids. There are also now laboratory scale observations (e.g. convection cells, surface solitons) and probable biological contexts.

5. In some cases rigorous bounds on the number of determining modes have recently been established (e.g. C. Foias, et. al., Phys. Rev. Lett. 50, 1031 (1983). Note also, in some cases (e.g. for certain reaction-diffusion problems), even a truncated set of linear modes can be accurate (J. C. Eilbeck, J. Math. Biol. 16, 233 (1983); B. Nicolaenko, et. al., Proc. Acad. Sc. Paris (1983)). It seems likely that the maximum number of modes is related to the fractal dimension. (O. Manley et. al., preprint, 1984, B. Nicolaenko and B. Scheurer, preprint, 1984).

6. e.g., R. K. Dodd, et. al. "Solitons and Nonlinear Wave Equations" (Academic Press 1982).

7. A. R. Bishop, et. al., Phys. Rev. Lett. 50, 1095 (1983), and references therein; and in Ref. 1; J. C. Eilbeck, Bull. I.M.A. (in press).

8. A. R. Bishop, et. al., APS March Meeting Bulletin (1984).
G. Wysin, et. al. APS March Meeting Bulletin (1984);

9. N. Ercolani, et. al., preprint (1983).

10. E. A. Overman, et. al., preprint (1984).

11. e.g. J. D. Farmer, et. al., Physica 7D, 153 (1983).

12. P. Grassberger and I. Procaccia, Phys. Rev. Lett. 50, 346 (1983). The calculation of various attractor "dimensions" remains in an early stage of development (see ref. 18). We emphasize that our error estimates here are deliberately conservative. Typically we used an embedding dimension of 8 and 8×10^4 data points.

13. Assuming only 2 breathers (or 4 kinks) as a truncated modal set, the maximum dimension of the space containing the attractor is 8. Our initial data symmetry reduces this to 4. The presence of dissipation will typically further reduce the "active" dimension. Our estimates of ν are generally in the range 2 - 2.5. This is entirely reasonable in view of our estimates (unpublished) of ν for a chaotic single particle with similar damping and driving strengths: there the maximum dimension is 2 but we generally find $\nu = 1.1 - 1.3$.

14. P. S. Lomdahl, et. al., Phys. Rev. B25, 5737 (1982).

Figure Captions

Figure 1. Space-time evolutions of $\phi(x,t)$ for the SG system (1) through two driving periods for $\varepsilon = 0.2$, $\omega_d = 0.6$, with periodic boundary conditions, and driving strengths a) $\gamma = 0.8$, which results in periodic time evolution, b) $\gamma = 1.0$, which results in motion nearly repeating every two driving periods.

Figure 2. Space-time evolutions of $\phi_t(x,t)$ for the SG system (1) through 1.6 driving periods for $\varepsilon = 0.1$, $\omega_d = 1.25$, with Neumann boundary conditions, D.C. driving $\gamma_0 = 0.35$, and A.C. driving strengths a) $\gamma = 1.2$, which produces a nonchaotic standing wave state on the third ZFS, b) $\gamma = 1.5$, which produces a pair of driven pulses.

Figure 3. Space-time evolutions of the in-plane angle $\phi(x,t)$ for the easy-plane ferromagnet (2) through two driving periods for $\varepsilon = 0.1$, $\omega_d = 0.05144$, with periodic boundary conditions, and driving strengths a) $B_0^x = .03429$, resulting in a standing wave pattern, b) $B_0^x = .02743$, resulting in intermittency between smooth standing wave structures and complicated breather-like patterns.

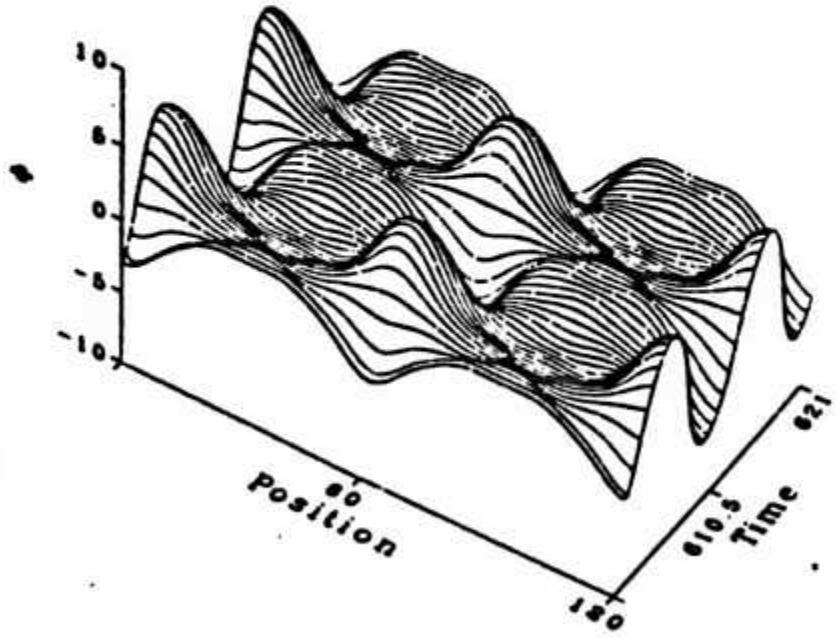
10
5
0
-5
-10
80
Position
180
1010.5
Time
1021

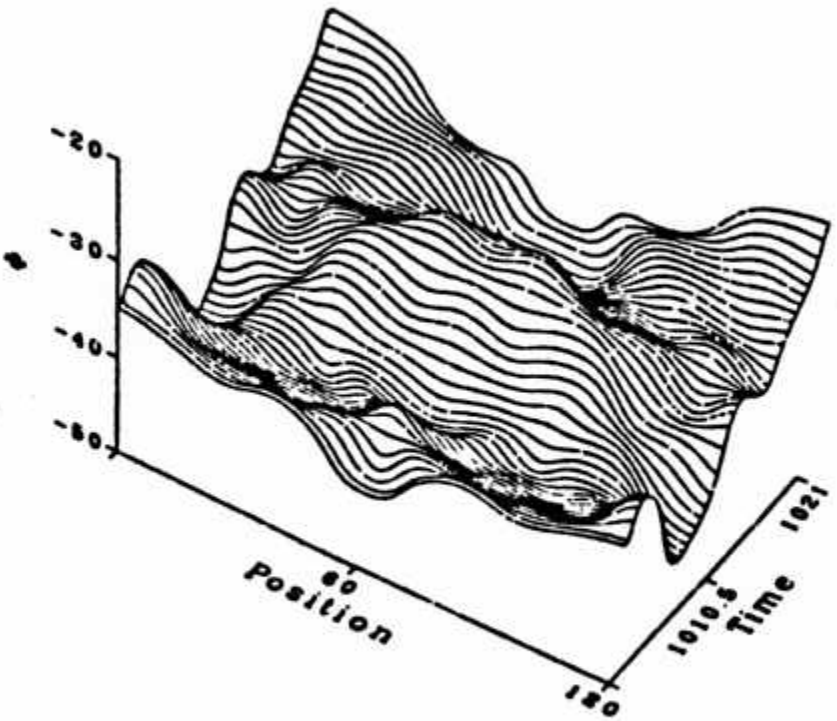
-20
-30
-40
-50
80
Position
180
1010.5
Time
1021

Fig 1

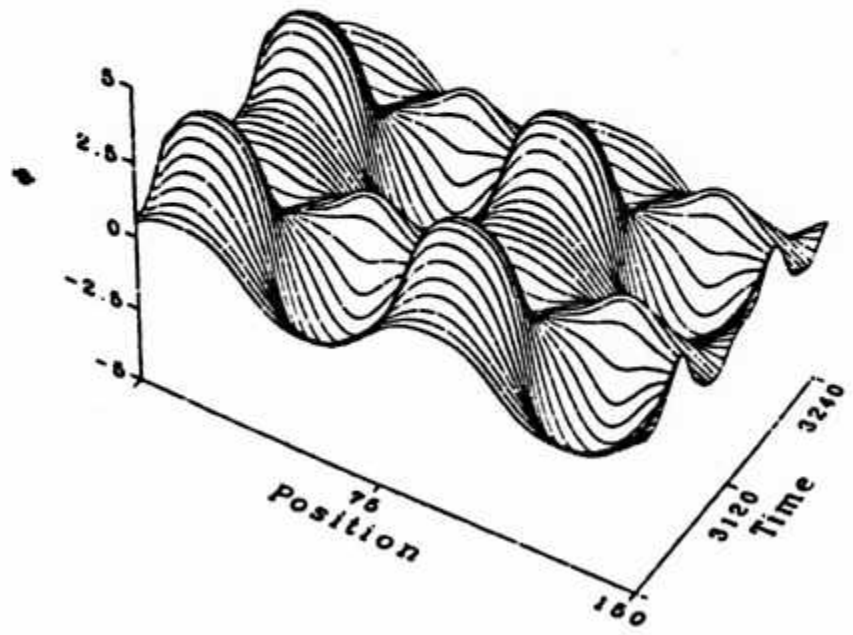
5
2.5
0
-2.5
-5
76
Position
160
3120
Time
3240

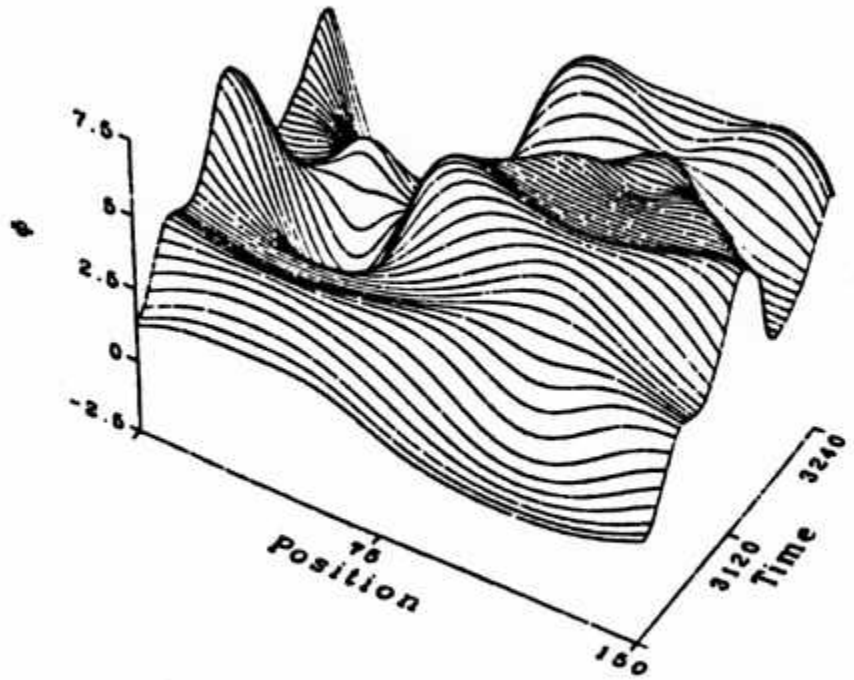
7.5
5
2.5
0
-2.5
76
Position
160
3120
Time
3240

FIG 2

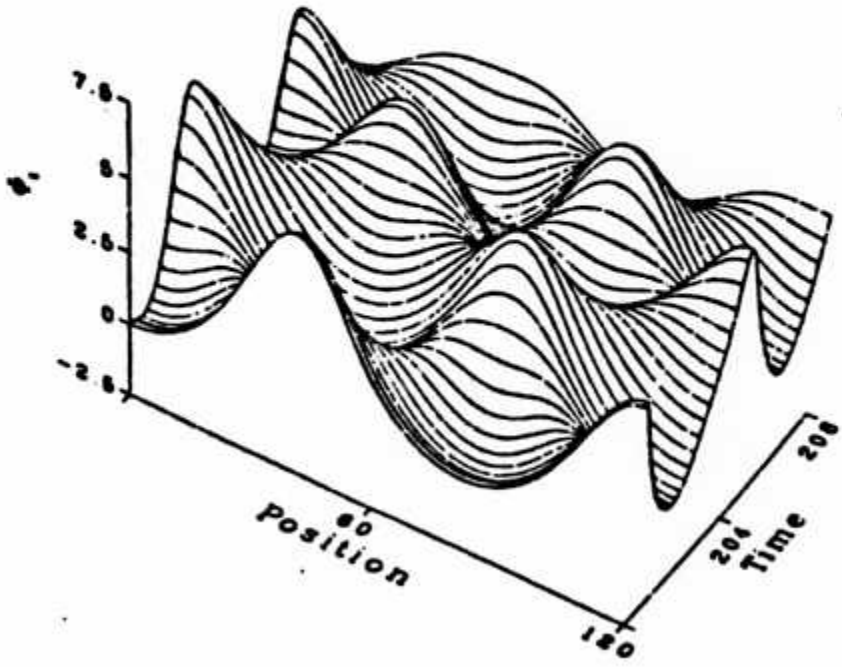
7.5
5
2.5
0
-2.5
Position
80
180
204
Time
208

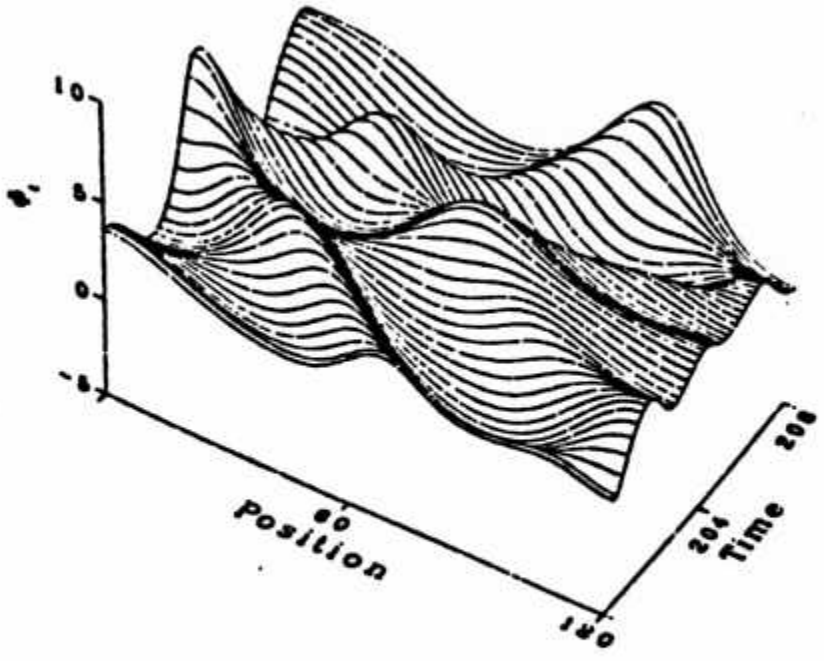
10
5
0
-5
Position
80
180
204
Time
208

FIG 3.